Article

Six-year-old ecological concrete in a marine environment: a case study

Amit Kenny [1,*] and Ela Ofer Rozovsky [2]

[1] Department of Civil Engineering, Shamoon College of Engineering, Ashdod, Israel; amitke@sce.ac.il
[2] Department of Civil Engineering, Ariel University, Ariel, Israel; e-mail@e-mail.com
* Correspondence: amit.kenny@gmail.com; Tel.: +972 52 4769952

Abstract: The durability of ecological concrete in a marine environment was studied. Specimens of a six-year-old submerged ecological concrete from a breakwater located in the East Mediterranean sea were analyzed for their biological carbonate deposition cover, chloride effective diffusion, carbonation, and mineralogy. About 57% of the surface was found to be covered by biogenic-deposited carbonates. The effective chloride diffusion coefficient and the carbonation rate were found to be reduced proportionally to the biogenic-carbonate cover. Most of the aluminates were found in non-crystalline minerals. No evidence of a sulfate attack was found.

Keywords: Ecological concrete; Cement/cementitious materials; Durability-related properties; Carbonation; Chloride; Diffusion;

List of notations

C	concentration / calcite in XRD
Cs	surface concentration
Ci	initial concentration in the concrete
D	diffusion coefficient / dolomite in XRD
Deff	effective diffusion coefficient
d	day
FA	fly-ash
G	gypsum
m	meter / time depended correction factor for effective diffusion
mm	mili-meter
P	paragonite
Q	quartz
SG	grounded granulated slag
s	second
t	time
tref	reference time
x	location measured from concrete surface
yr	year
ω	water to cement ratio

1. Introduction

The durability of reinforced concrete structures (RCS) in marine and coastal environments is a major concern. Three main processes degrade RCS: (1) chloride diffusion, which leads to steel reinforcement corrosion; (2) carbonation, which causes pH reduction and therefore leads to steel reinforcement corrosion; and (3) sulfate attack, which causes a deterioration of the cement paste of the concrete itself. In real-life conditions, most of the structures in marine and coastal environments are initially damaged by steel corrosion

 doi:10.20944/preprints202212.0241.v1

caused by chloride diffusion, which in most cases occurs at a rate higher than those of the carbonation and sulfate attacks.

To mitigate chloride-induced corrosion in RCS, different solutions have been proposed. The main approach in most of these solutions is to reduce the permeability of concrete for chloride ingress. The common engineering measure of chloride permeability is the effective diffusion coefficient (D_{eff}). It was shown that by reducing the D_{eff}, the time it takes for chloride concentration at the rebar depth to reach a critical concentration in which steel corrosion initiates increases. The D_{eff} can be used to estimate this time and so allows prediction of the service life of the RCS.

According to Ehlen [1] and other research groups [2–4], D_{eff} is influenced mainly by the following three parameters: (1) the water-to-cement ratio (W/C), (2) the use of supplementary cementitious materials (SCMs), and (3) the degree of hydration of the cement paste. A lower W/C ratio reduces the D_{eff} [1]. The use of SCMs reduces the D_{eff} for concretes that have the same strength at the age of 28 days [5]. As the degree of hydration increases, the D_{eff} decreases. D_{eff} is also temperature-dependent and increases with increasing temperature [1].

A software package called Life365 [1] is a calculative tool for the prediction of RCS service life in chloride-induced environments. For its calculation, the software can estimate D_{eff} based on models incorporating binder composition, W/C ratio, and time [1]; or it can use measured data, such as data from a standard method of D_{eff} assessment, the ASTM C 1556 [6]. The ASTM C 1556 method uses curve fitting of the chloride profile measurements from a laboratory specimen to the unidirectional diffusion equation for its D_{eff} determination [6].

However, this method ignores the carbonation and the sulfate attack processes and does not predict their rates. One of the reasons is that the carbonation depth prediction model in [7–9] shows that the carbonation rate decreases drastically in very high humidity conditions. Hence, it can be estimated that the carbonation rate in seawater and in the spray zone is predicted to be low, although the models in this work do not include the submarine environment and exclude consideration of the cement composition of the concrete. The existing sulfate attack models [10,11] are commonly calibrated for ordinary Portland cement (OPC), hence are not adequate for the prediction of damage of slag-based marine concrete.

Ecological marine concrete is a concrete, which due to its textured surface and the addition of appropriate additives, encourages sessile marine organisms to settle on the concrete surface. This is in contrast with common concrete, which remains poorly inhabited for decades [19,20]. The introduction of a new mineral additive for ecological marine concrete by EConcrete™ raised concerns regarding the influence of the marine biota's adherence to the concrete on the durability of the RCS. Some former works investigated the influence of marine sessile organisms on parameters of concrete durability [12–17]. It was shown that sessile carbonate-depositing organisms create a dense carbonate coverage on the concrete surface in the spots where they attach to the surface. This deposition seals the concrete surface like a membrane, and reduces the effective diffusion of chloride through the concrete [12]. These works investigated the settlement on common concrete, which may have lower coverage of sessile carbonate-depositing organisms relative to those that may be found on ecological concrete. The question is whether this bio-protection changes the rates of chloride ingress, carbonation, and sulfate attack.

The determination of the Deff, as well as the assessment of the carbonation and sulfate attack rates in real structures made of ecological concrete, is important for the prediction of the durability of any novel RCS. In this work, specimens from ecological concrete from a 6-year-old breakwater antifer (Figure 1), a component of a breakwater, were analyzed. The antifer was located on the coast of Haifa, Israel, at a depth of 9 meters; two cores were drilled from it 6 years after it was cast. A chloride concentration profile was measured using ASTM C 1556 method on these cores to retrieve the Deff. For validation of the model used for the durability estimation, the Deff was compared to data simulated by the Life365 program. XRDs of samples from different depths of the concrete surface

Preprints (www.preprints.org) | NOT PEER-REVIEWED | Posted: 14 December 2022 doi:10.20944/preprints202212.0241.v1

were carried out. The carbonation rate was measured by the phenolphthalein method. The biological carbonation coverage was estimated. The relation of the parameters relevant for durability with the biogenic coverage was investigated.

Figure 1. The antifers before placement in the breakwater.

2. Materials and Methods

Two cores, each 95 mm in diameter, were drilled out of a six-year-old breakwater antifer at a depth of 9 meters located on the coast of Haifa, Israel (Figure 2). The ecological concrete composition used for the cast antifer is shown in Table 1. The ecological additive EcoP is a mixture of minerals, mostly based on calcium and silica with only 10% pozzolanic material. One core was pulverized on a lathe. Samples at every 1 mm interval were collected for analysis. The second core was used for carbonation depth measurement.

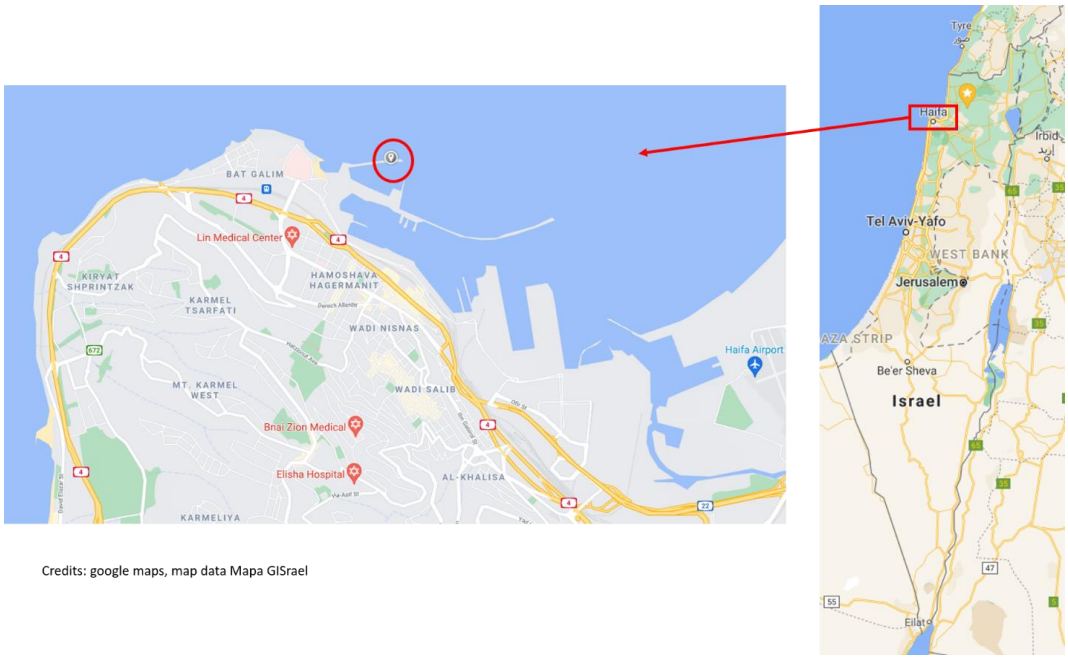

Figure 2. Exposure location, Haifa, Israel

Table 1. Concrete mix

Ingredient	Kg/m^3

Preprints (www.preprints.org) | NOT PEER-REVIEWED | Posted: 14 December 2022 doi:10.20944/preprints202212.0241.v1

14-19 mm aggregate	830
9-14 mm aggregate	409
0-9 mm aggregate	374
Sand	374
Water	140
Cement CEM III B 42.5 N[1]	260
EcoP ecological additive[2]	60

[1] according to EN-197, contains 20-34% clinker and 66-80% slag
[2] a commercial additive by EConcrete™

2.1 Estimation of biogenic carbonate coverage

The surface of the face of one core was cleaned by using a plastic brush with hard hairs together with a commercial diluted sodium hypochlorite solution (bleach). The face was photographed with Nikon Coolpix AW100 on a colored cardboard background (Figure 3 a). Several distinct surfaces can be detected: concrete (with a reddish tan due to algae), shell valves, and shells of sessile gastropods of the Vermetidae family [18] in various sizes. The image was clustered by the k-means algorithm into 4 clusters (Figure 3 c). Each cluster was classified into background, concrete, and biogenic carbonate deposition (Figure 3 d). The biogenic carbonate coverage was estimated by dividing the number of biogenic carbonate pixels, bc, by the not background pixels, conc, i.e. pixels of concrete surface.

$$coverage = \frac{bc}{conc} \quad (1)$$

(a)

(b)

Preprints (www.preprints.org) | NOT PEER-REVIEWED | Posted: 14 December 2022 doi:10.20944/preprints202212.0241.v1

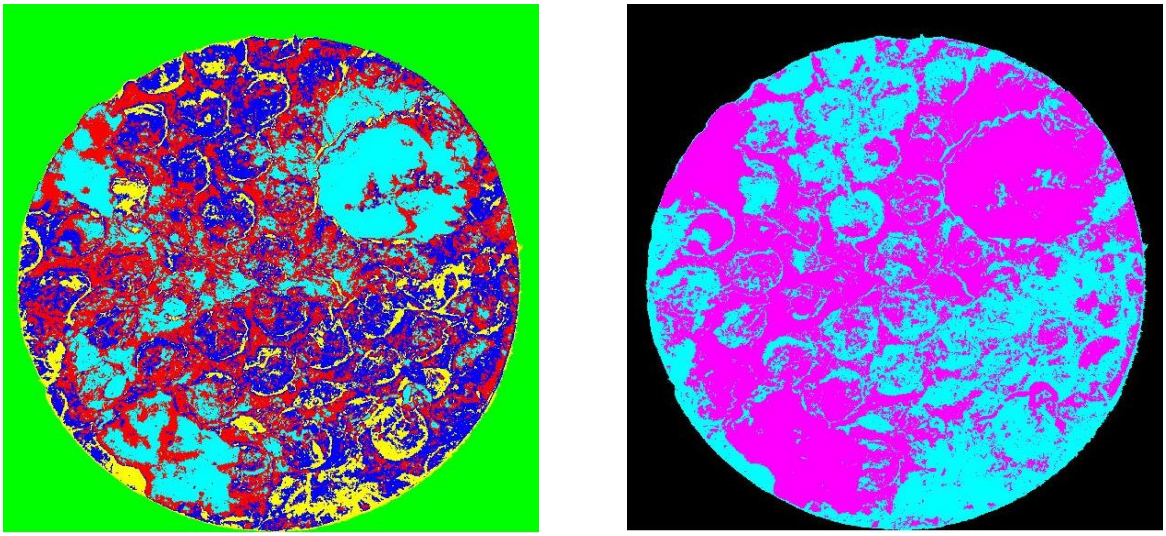

(c) (d)

Figure 3. A 95 mm core for carbonate coverage analysis. (a) original with a cardboard background. (b) background removed. (c) clustered image. (d) classified image, magenta - biogenic carbonate deposition.

2.2 Chloride profile measurement

After pulverization, the concrete powder was analyzed according to ASTM C 1152 after appropriate dilution. The chloride concentration in the solution was measured by the chloride ion-selective electrode (ISE) by Pasco™. ISE allows measurement of low volume samples with a wide range of sensitivities (10^{-1} M -10^{-5} M).

2.3 Diffusion coefficient estimation

The diffusion coefficient was estimated by fitting the data to the unidirectional diffusion equation according to ASTM C 1556,

$$C(x,t) = C_s - (C_s - C_i) \cdot erf\left(\frac{x}{\sqrt{4 \cdot D_{eff} \cdot t}}\right) \quad (2)$$

where $C(x,t)$ is the chloride concentration measured at depth, x, and time , t, C_s is the projected chloride concentration at the interface between the exposure liquid and the concrete, C_i is the initial chloride concentration in the concrete before submersion, x is the depth from the exposure surface, t is the time from exposure, D_{eff} is the effective diffusion coefficient (also known as apparent diffusion coefficient), and erf is the error function.

The curve fitting was performed using a MATLAB curve fitting tool (CF tool).

2.4 XRD analysis

The XRD analysis of samples from several intervals (1, 6, 7, 10, 14, 19, and 26 mm) was conducted using a Rigaku SmartLab SE diffractometer with CuKα radiation at 40 kV, 30 mA, and a scanning speed of 0.02° min-1. In all cases, measurements were conducted from 2θ=5° to 2θ=120°, but data in the range of 2θ=70°-120° did not yield much information and therefore was omitted from the presentation for the sake of clarity. The program used for received scans was SmartLab Studio II v4.2.44.0, the program for diffraction

Preprints (www.preprints.org) | NOT PEER-REVIEWED | Posted: 14 December 2022 doi:10.20944/preprints202212.0241.v1

pattern analysis was X'Pert HighScore Plus v2.2e, and the database was taken from ICDD PDF-2 (2009 release). Semi-Rietveld analysis was performed.

2.5 Carbonation rate

Carbonation depth was measured 953 days after drilling by the phenolphthalein method. Since the concrete face is irregular (Figure 3), red putty was used to mark the concrete face. 21 spots were measured from the face, and 49 from the cylinder edge (Figure 4).

Figure 4. Halved core sprayed with phenolphthalein after exposure to air for 953 Days

3. Results and Discussion

3.1 Estimation of biogenic carbonate cover

The original image and its classification are shown in Figure 3. The measurements done according to equation 1 showed that the relative area covered by biogenic calcium carbonate deposits is 56.6%.

3.2 Chloride profile

The chloride concentration-to-concrete weight decreased as a function of depth within the antifer (Figure 5). The fitting curve to this relation was taken from eq. 2 in ASTM C1152. Experimental data below 5 mm depth were scattered, as in this region the surface is uneven (Figure 6 b and Figure 1) and the distribution of aggregates is not homogenous. Furthermore, a lower cement paste concentration was measured (Figure 6 a). Since the chloride ions penetrate only the paste, lower chloride concentrations are expected in areas with lower paste content. The fitting parameters, i.e. surface concentration (C_s), initial concentration (C_i), effective diffusion coefficient (D_{eff}) and accuracy of fitting to unidirectional diffusion, are listed in Table 2. Very good fitting indicators are obtained, as the R^2 value is close to 1 (0.97), and the SSE (sum of square error) and RMSE (residual mean square error) values are quite low (0.112 and 0.075, respectively), indicating that diffusion is the main chloride ingress mechanism in the seawater-immersed ecological concrete.

The initial chloride concentration of the concrete C_i is practically zero. Such a result may be an artifact of the diffusion coefficient's change with time, as has been demonstrated by Pack et al. [19] in simulations. The surface chloride concentration, C_s, is about 2 gr/kg which is lower than the values found in the literature for tidal zones (8 in [1] and 2.9-5.9 gr/kg in [20]). Lower surface chloride concentration may be a result of lower surface area due to biogenic carbonate coverage. The diffusion coefficient obtained from the experimental results and according to ASTM C1152 is $7.5 \cdot 10^{-13}$ m^2/s.

Our next question was: is this diffusion coefficient value the same as that in concrete with no biogenic cover, or does the coverage decrease the chloride diffusion? In order to estimate the diffusion coefficient of the sampled ecological concrete, we calculated the expected D_{eff} according to the assumptions in LIFE-365 [1]:

Preprints (www.preprints.org) | NOT PEER-REVIEWED | Posted: 14 December 2022 doi:10.20944/preprints202212.0241.v1

$$D(28day) = 10^{-12.06+2.4\cdot\omega}\ \frac{m^2}{\text{sec}} \tag{3}$$

$$D(t) = D_{ref}\cdot\left(\frac{t_{ref}}{t}\right)^{m} \tag{4}$$

$$m = 0.2 + 0.4\cdot\left(\frac{\%FA}{50} + \frac{\%SG}{70}\right) \tag{5}$$

where D is the effective diffusion coefficient, ω is the water-to-cement ratio, t the time, FA fly-ash, and SG slags. Eco-P additive was considered as an inert filler with only 10% pozzolanic material, FA. It was added as FA to eq. 5. This simulation allows the estimation of the diffusion coefficient after different periods. The resulting D_{eff} after 28 days and 6 years under an assumption of a fixed temperature of 20°C is shown in Table 3. The expected D_{eff} for this ecological concrete formed mainly from slags is $1.12\cdot10^{-12}$ m²/s after 6 years. The experimental value obtained ($7.5\cdot10^{-13}$ m²/s) was 67% of this value, indicating that the diffusion coefficient had decreased due to biogenic carbonate coverage which was estimated to be close to 60% by optic means. It is interesting to note that a similar trend appeared in the research of Kawabata et al., where a diffusion coefficient of $1.68\cdot10^{-12}$ m²/sec was found in concrete with no organisms on it, while specimens with about 50% coverage of organisms had 30-60% of this value, i.e. $5.04\cdot10^{-13}$ to $1.01\cdot10^{-12}$ m²/sec [12]. This proves that a biological settlement on marine concrete improves its durability.

Table 2. Parameters and indicators for the goodness of fit for a chloride profile unidirectional diffusion model. Data below 5 mm excluded; C_s – surface concentration; C_i – original concentration in concrete; D_{eff} – effective diffusion coefficient; limits are for 95% confidence. SSE - Sum squared error performance function, RMSE - root-mean-square error.

Parameter	Value
C_s (gr/kg)	2.07 ±0.13
C_i (gr/kg)	0 * ±2.22e-14
D_{eff} (m^2s^{-1})	7.5e-13 ±1.0e-13
SSE	0.1118
R^2	0.9701
RMSE	0.07477

* C_0 is defined as a positive value

Preprints (www.preprints.org) | NOT PEER-REVIEWED | Posted: 14 December 2022 doi:10.20944/preprints202212.0241.v1

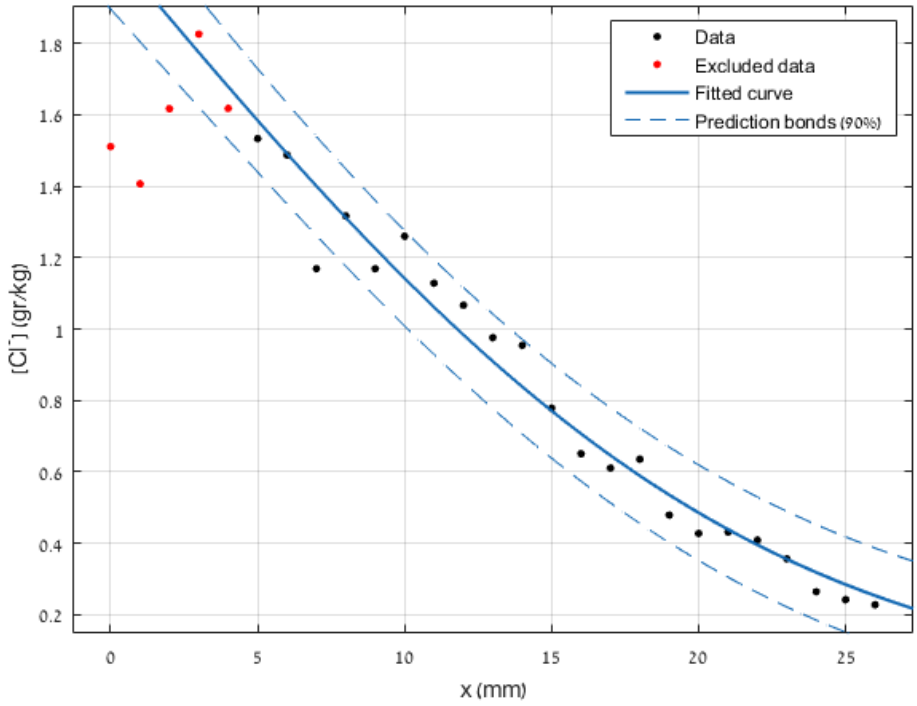

Figure 5. Chloride profile (experimental) and unidirectional diffusion model fitting.

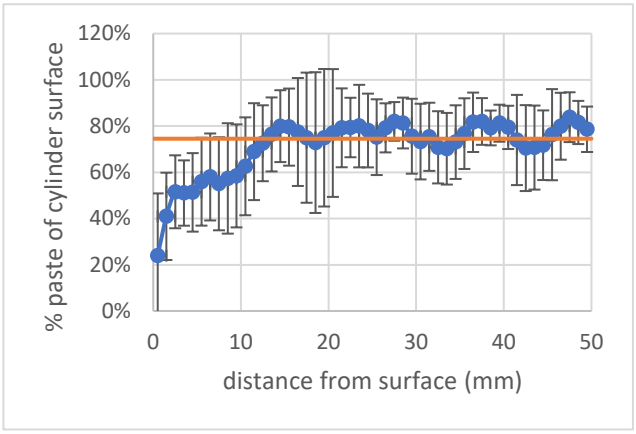

(a) (b)

Figure 6. Sources for variation of chloride concentration at low depth. (a) Paste concentration from image processing of the sides of the core was used for carbonation depth measurement. The orange line is the paste concentration in the concrete calculated from the concrete mix composition. (b) Image of the surface of the core used for carbonation depth measurement.

Table 3. Calculation of D_{eff} based on equations 3-5 in [1]

W/C	0.53
SG (%)	68.40
FA[1] (%)	2.25
D_{eff} at 28d (m^2/sec)	1.60E-11
m	0.61

 doi:10.20944/preprints202212.0241.v1

D_{eff} at 6yr (m^2/sec)	1.12E-12

[1] Eco-P is calculated as FA

3.3 Carbonation

Unfortunately, the carbonation test was performed just 953 days after drilling, but it can be assumed that during the time the specimen was submerged in seawater no carbonation occurred. After opening the drilled specimen, regular carbonation for a 953-day exposure to air was observed. Carbonation depth measured was 7.5 ±1.7 mm for the face of the antifer which was external (i.e., covered by sessile organisms), and 14.6 ±3 mm for the other sides (Figure 4). This yields a carbonation rate of 4.6 mm·yr$^{-½}$ for the face and a higher rate of 9.2 mm·yr$^{-½}$ for the sides where no sessile organisms were developed. The ratio between the carbonation rates is 2, which corresponds with the biogenic carbonate coverage of the face as found in the image-based estimation.

3.4 XRD

Results of the XRD of samples from different depths are shown in Figure 7. The corresponding peak analysis is shown in Table 4. XRD spectra were normalized with respect to the calcite diffraction line at 2θ=29.405°, as according to semi-Rietveld analysis its quantity is similar in all powders (7±1%). Close to the surface (1 mm), a higher amount of sand (quartz) is indeed detected, while at higher depths the quantities of dolomite from the coarse aggregates and quartz from the sand is similar in all the tested samples. This is another indication that the first 5 mm needs to be omitted from the results similarly to that done for the unidirectional diffusion curve.

Ettringite and thaumisite, two common sulfate-containing minerals in concrete, were not detected by XRD, indicating that sulfates did not incorporate into the crystalline structures. This is even though the Mediterranean Sea contains 1,920-3,840 ppm SO_4^{-2} [21], while at the depth of 0.5 meters a concentration of 2,880 ppm was measured [22]. The absence of these phases probably results from the absence of C_3A hydrates in the hydrated cement of the ecological concrete. Another sulfate-containing crystal, gypsum, was detected in low concentrations. It is not clear whether the sulfates were part of the original concrete mix, or penetrated later and reacted with calcium hydroxide from the cement paste. If the sulfate came from the seawater, a concentration drop with depth is expected, as the results indeed show. This drop can have two explanations: (1) lower sulfate diffusion in greater depths of the concrete; (2) reduction of the sulfate on the concrete surface by sulfate-reducing bacteria which develop as a biofilm on the concrete surface. Such a bacteria may hinder the ingress of additional sulfates as can be seen in sediments, where the sulfate concentration decreases with depth [21]. These explanations are speculative and should be investigated experimentally.

Small amounts of crystalized aluminate phase were detected in some samples. It can be inferred that the aluminate phases in the ecological concrete are mostly amorphous.

Preprints (www.preprints.org) | NOT PEER-REVIEWED | Posted: 14 December 2022 doi:10.20944/preprints202212.0241.v1

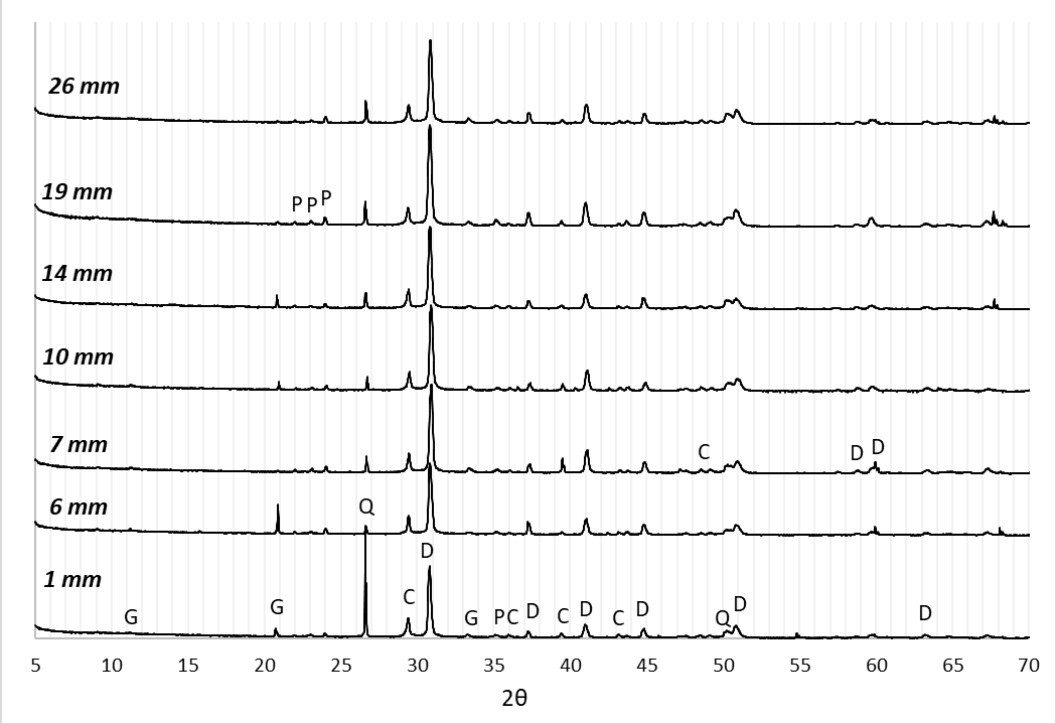

Figure 7: X-ray diffraction of powders from different depths of the breakwater. The definition of the capital letters appears in Table 4.

Table 4: Semi-quantitative analysis of powders from different depths

Mineral name	PDF card	26 mm	19 mm	14 mm	10 mm	7 mm	6 mm	1 mm	
Dolomite (D)	01-074-1687	90%	90%	88%	85%	88%	88%	79%	$(CaMg)(CO_3)_2$
Calcite (C)	01-086-2334	6%	6%	6%	8%	8%	6%	8%	$CaCO_3$
Quartz (Q)	01-085-0795	3%	4%	3%	2%	3%	2%	10%	SiO_2
Gypsum (G)	98-011-422	ND	ND	2%	3%	1%	3%	2%	$CaSO_4{\cdot}2H_2O$
Paragonite 2M1 (P)	01-075-1202	1%	ND	1%	2%	ND	1%	1%	$NaAl_2(AlSi_3O_{10})(OH)_2$

4. Conclusions

- In the case studied here, sessile marine organisms improved the durability of reinforced concrete structures.
- The effective ingress of chlorides and carbonates was reduced in proportion to the concrete coverage by the sessile carbonate-depositing organisms that had formed on the ecological concrete.
- The Deff of chlorides of the ecological concrete investigated is equal to or lower than the expected Deff of similar concrete calculated in models in the literature.
- The marine ecological concrete did not undergo sulfate attack.
- During coastal development, ecological concrete should be considered, as it has ecological and long-term performance benefits as compared to ordinary concrete.

Author Contributions: Conceptualization, A. Kenny; methodology, A. Kenny and E. Ofer Rozovsky; software, A. Kenny; investigation, A. Kenny and E. Ofer Rozovsky; resources, A. Kenny and E. Ofer Rozovsky; data curation, A. Kenny; writing—original draft preparation, A. Kenny and E. Ofer Rozovsky; writing—review and editing, A. Kenny and E. Ofer Rozovsky. All authors have read and agreed to the published version of the manuscript.

Funding: This research received no external funding

Data Availability Statement: DOI: 10.13140/RG.2.2.30182.91200

Acknowledgments: The authors thank EConcrete™ for supplying the specimens and concrete mix data for this study.

Conflicts of Interest: A. Kenny serves as an external consultant to EConcrete™.

References

[1] M.A. Ehlen, Life-365 Service Life Prediction Model and Computer Program for Predicting the Service Life and Life-Cycle Cost of Reinforced Concrete Exposed to Chlorides, (2009).
[2] M. Shi, Z. Chen, J. Sun, Determination of chloride diffusivity in concrete by AC impedance spectroscopy, Cem. Concr. Res. 29 (1999) 1111{}--1115.
[3] F. Lollini, E. Redaelli, L. Bertolini, Investigation on the effect of supplementary cementitious materials on the critical chloride threshold of steel in concrete, Mater. Struct. Constr. 49 (2016) 4147–4165. https://doi.org/10.1617/s11527-015-0778-0.
[4] S.E. Chidiac, M. Shafikhani, Phenomenological model for quantifying concrete chloride diffusion coefficient, Constr. Build. Mater. 224 (2019) 773–784. https://doi.org/10.1016/J.CONBUILDMAT.2019.07.006.
[5] F. Massazza, Pozzolana and Pozzolanic Cement, in: P.C. Hewlett (Ed.), LEA's Chem. Cem. Concr., Fourth, Arnold, 1998: pp. 471–632.
[6] H. Friedmann, O. Amiri, A. Aït-Mokhtar, P. Dumargue, A direct method for determining chloride diffusion coefficient by using migration test, Cem. Concr. Res. 34 (2004) 1967–1973. https://doi.org/10.1016/J.CEMCONRES.2004.01.009.
[7] P. Liu, Z. Yu, Y. Chen, Carbonation depth model and carbonated acceleration rate of concrete under different environment, Cem. Concr. Compos. 114 (2020) 103736. https://doi.org/10.1016/J.CEMCONCOMP.2020.103736.
[8] T.P. Hills, F. Gordon, N.H. Florin, P.S. Fennell, Statistical analysis of the carbonation rate of concrete, Cem. Concr. Res. 72 (2015) 98–107. https://doi.org/10.1016/J.CEMCONRES.2015.02.007.
[9] V.L. Ta, S. Bonnet, T. Senga Kiesse, A. Ventura, A new meta-model to calculate carbonation front depth within concrete structures, Constr. Build. Mater. 129 (2016) 172–181. https://doi.org/10.1016/J.CONBUILDMAT.2016.10.103.
[10] S. Qin, D. Zou, T. Liu, A. Jivkov, A chemo-transport-damage model for concrete under external sulfate attack, Cem. Concr. Res. 132 (2020) 106048. https://doi.org/10.1016/J.CEMCONRES.2020.106048.
[11] J.K. Chen, C. Qian, H. Song, A new chemo-mechanical model of damage in concrete under sulfate attack, Constr. Build. Mater. 115 (2016) 536–543. https://doi.org/10.1016/J.CONBUILDMAT.2016.04.074.
[12] Y. Kawabata, E. Kato, M. Iwanami, Enhanced long-term resistance of concrete with marine sessile organisms to chloride ion penetration, J. Adv. Concr. Technol. (2012). https://doi.org/10.3151/jact.10.151.
[13] M.A. Coombes, H.A. Viles, L.A. Naylor, E.C. La Marca, Cool barnacles: Do common biogenic structures enhance or retard rates of deterioration of intertidal rocks and concrete?, Sci. Total Environ. 580 (2017) 1034–1045. https://doi.org/10.1016/J.SCITOTENV.2016.12.058.
[14] M.A. Coombes, L.A. Naylor, H.A. Viles, R.C. Thompson, Bioprotection and disturbance: Seaweed, microclimatic stability and conditions for mechanical weathering in the intertidal zone, Geomorphology. 202 (2013) 4–14. https://doi.org/10.1016/j.geomorph.2012.09.014.
[15] T. Chlayon, M. Iwanami, N. Chijiwa, Combined protective action of barnacles and biofilm on concrete surface in intertidal areas, Constr. Build. Mater. 179 (2018) 477–487. https://doi.org/10.1016/J.CONBUILDMAT.2018.05.223.
[16] T. Chlayon, M. Iwanami, N. Chijiwa, Impacts from concrete microstructure and surface on the settlement of sessile organisms affecting chloride attack, Constr. Build. Mater. 239 (2020) 117863. https://doi.org/10.1016/J.CONBUILDMAT.2019.117863.
[17] P. Hughes, D. Fairhurst, I. Sherrington, N. Renevier, L.H.G.G. Morton, P.C. Robery, L. Cunningham, Microscopic study into biodeterioration of marine concrete, Int. Biodeterior. Biodegrad. 79 (2013) 14–19. https://doi.org/10.1016/j.ibiod.2013.01.007.
[18] M. Di Monterosato, Nomenclatura generica e specifica di alcune conchiglie mediterraneeTitle, Palermo, 1884. https://www.biodiversitylibrary.org/item/109711#page/1/mode/1up.
[19] S.W. Pack, M.S. Jung, H.W. Song, S.H. Kim, K.Y. Ann, Prediction of time dependent chloride transport in concrete structures exposed to a marine environment, Cem. Concr. Res. (2010). https://doi.org/10.1016/j.cemconres.2009.09.023.
[20] A. Costa, J. Appleton, Chloride penetration into concrete in marine environment—Part I: Main parameters affecting chloride penetration, Mater. Struct. 32 (1999) 252–259. https://doi.org/10.1007/BF02479594.

 doi:10.20944/preprints202212.0241.v1

[21] M. Sela-Adler, B. Herut, I. Bar-Or, G. Antler, E. Eliani-Russak, E. Levy, Y. Makovsky, O. Sivan, Geochemical evidence for biogenic methane production and consumption in the shallow sediments of the SE Mediterranean shelf (Israel), Cont. Shelf Res. 101 (2015) 117–124. https://doi.org/10.1016/J.CSR.2015.04.001.
[22] B. HERUT, A. STARINSKY, A. KATZ, A. BEIN, The role of seawater freezing in the formation of subsurface brines, Geochim. Cowmchimica Acta. 54 (1990) 13–21.
: URL (accessed on Day Month Year).